The effects of organophosphorus insecticides and heavy metals on DNA damage and programmed cell death in two plant models

Josefina Cortés-Eslava[a], Sandra Gómez-Arroyo [a*], Maria C. Risueño[b], Pilar S. Testillano[b]

[a]*Laboratorio de Genotoxicología Ambiental, Centro de Ciencias de la Atmósfera, Universidad Nacional Autónoma de México, Ciudad Universitaria, Coyoacán 04510 Ciudad de México, México.*

[b]*Laboratory of Pollen Biotechnology of Crop Plants, Centro de Investigaciones Biológicas (CIB), C.S.I.C., Ramiro de Maeztu, 9, 28040 Madrid, España.*

Josefina Cortés Eslava jcortes@atmosfera.unam.mx
María C. Risueño risueno@cib.csic.es
Pilar S. Testillano testillano@cib.csic.es
Sandra Gómez Arroyo slg@atmosfera.unam.mx

Corresponding author. Tel.: +52 55 5622 4051, fax +52 55 5616 0789. E. mail address: slga@atmosfera.unam.mx

Keywords: Malathion, Fenthion, Chromium, Nickel, Genotoxicity, Apoptotic-like-Programmed Cell Death (AL-PCD), *Allium cepa*, *Vicia faba*,

The authors declare that any of them have commercial interest in the methods neither results of this research.

ABSTRACT:

The ubiquity of pollutants, such as agrochemicals and heavy metals, constitute a serious risk to human health. To evaluate the induction of DNA damage and programmed cell death (PCD), root cells of *Allium cepa* and *Vicia faba* were treated with two organophosphate insecticides (OI), fenthion and malathion, and with two heavy metal (HM) salts, nickel nitrate and potassium dichromate. An alkaline variant of the comet assay was performed to identify DNA breaks; the results showed comets in a dose-dependent manner, while higher concentrations induced clouds following exposure to OIs and HMs. Similarly, treatments with higher concentrations of OIs and HMs were analyzed by immunocytochemistry, and several structural characteristics of PCD were observed, including chromatin condensation, cytoplasmic vacuolization, nuclear shrinkage, condensation of the protoplast away from the cell wall, and nuclei fragmentation with apoptotic-like corpse formation. Abiotic stress also caused other features associated with PCD, such as an increase in the presence of active caspase-3-like protein, changes in the

location of cytochrome C (Cyt C) toward the cytoplasm, and decreases in extracellular signal-regulated protein kinase (ERK) expression. Genotoxicity results allow setting out an oxidative stress via of DNA damage and the role of the high affinity of HM and OI by DNA molecule as underlying cause of genotoxic effect. The PCD features that were observed in root cells of *A. cepa* and *V. faba* suggest that PCD takes place through a process that involves ERK inactivation, which culminates in cytochrome c release and caspase-3-like activation. The sensitivity of both plant models to abiotic stress was clearly demonstrated, validating their role as good biosensors of DNA breakage and PCD induced by environmental stressors.

Capsule:
Insecticides phenthion and malathion, and the salts nickel nitrate and potassium dichromate cause genotoxic damage and apoptotic-like effects in *Vicia faba* and *Allium cepa*.

1. INTRODUCTION

Harmful environmental stressors (such as cytotoxic agents, pollutants, and toxicants) are well known to induce genotoxicity (Møller et al., 2015) and apoptotic cell death, and to contribute to a variety of pathological conditions (Slotkin and Seidler, 2012). Organophosphorus insecticides (OIs) and heavy metals (HMs) are pollutants that are extensively released in the environment, and they are therefore a potential risk to human health. There is widespread application of pesticides to control pests and diseases that attack agricultural products. Since organochlorine insecticide were removed from usage, organophosphorus insecticides have become the most widely used compounds available.

Plants are capable of bio-concentrating environmental agents and activating pro-mutagens into toxic metabolites that introduce new mutagens into the human food chain (Cortés-Eslava et al., 2013). Malathion and fenthion are two OIs that are commonly used in agriculture in developing countries (Tsatsakis et al., 2008). Berrada et al. (2006) detected residues of both compounds in oranges, tangerines, apricots, nectarines, persimmons, and watermelons collected from agricultural valleys of Valencia, Spain. Numerous health impacts have been reported following exposures to fenthion and malathion.

HMs can also cause serious ecotoxicological problems because they are non-degradable and they persist in the environment (Rana, 2008). Chromium $(Cr)^{-}$ and nickel $(Ni)^{-}$ mediated toxicity, reported by Lou et al. (2013), involve oxidative DNA damage, lipid peroxidation, and changes in calcium and sulfhydryl homeostasis. Ni produces reactive oxygen species (ROS) ($^{\circ}OH^{-}$), lipid peroxidation, and oxidative stress (Chervona and Costa, 2012). Both Cr and Ni produce toxic, mutagenic, and carcinogenic effects in biological systems (Kuo et al., 2006; Palaniappan and Karthikeyan, 2009). Apoptotic pathways mediated by ROS, mitochondria, endoplasmic reticulum (ER), Fas, and cMyc participate in Ni-induced cell apoptosis; however, the exact mechanism of apoptosis caused by Ni is still unclear.

In general, plant bioassays are more sensitive than most other systems in terms of detecting genotoxic effects caused by environmental pollutants. They have been extensively used because they are inexpensive, quick and easy to run the assays (Ma, 1999). The first reports on the use of the comet assay in plants date from 1990s (Gichner and Plewa, 1998; Koppen and Verschaeve, 1996; Navarrete et al., 1997). This fluorescent technology is sensitive for the detection of single- or double-chain DNA breaks, the detection of alkali-labile sites, and the presence of cross-linked protein-DNA with high reproducibility. Plant protocols for this unicellular methodology take in account relevant differences to other eukaryotic systems, including the presence of a rigid cell wall in plant cells. In the last decade, the use of the plant comet assay has drastically increased in the systematic study of the induction of genotoxicity, mutagenicity, and PCD following exposure to pollutants and other stress agents, which highlights its relevance and utility (Santos et al., 2015).

PCD constitutes a sequence of events that lead to the genetically controlled and organized destruction of the cell (Lockshin and Zakeri, 2004). It is an integral part of plant development and of responses to biotic and abiotic stressors and pathogens (Rodríguez-Serrano et al., 2012; Solís et al., 2014; van Doorn et al., 2011). Morphologically defined PCD in plants should be termed apoptotic-like PCD (AL-PCD) (Reape et al., 2008). The use of this term acknowledges that there are similarities between AL-PCD and apoptosis, while recognizing that there are distinct, and perhaps fundamental differences (Reape and McCabe, 2010). In plants, AL-PCD is distinguished from other forms of plant cell death by

protoplast condensation away from the cell wall, which results in morphologically distinct cell corpses and DNA degradation. In addition, there is a central regulatory role for the mitochondria and the degradation of the cell and its contents by PCD-associated proteases (Reape et al., 2008).

In plants, mitogen-activated protein kinases (MAPK) play diverse roles in intra- and extracellular signaling; this protein kinase cascade is involved in the transduction of diverse extracellular stimuli, such as biotic and abiotic stressors, pathogen infections, heavy metals, pesticides, wounding, high and low temperature, high salinity, ultraviolet radiation, ozone, ROS, drought, and high or low osmolality (Taj et al., 2010). The extracellular signal-regulated protein kinases (ERKs), a type of MAPK protein, is related to proliferation and differentiation in various animal and plant systems (Seguí-Simarro et al., 2005). The involvement of MAPKs and DNA repair network underlie aluminum-induced DNA damage and adaptive responses to genotoxic stress in the root cells of *A. cepa* (Panda and Achary, 2014). Genotoxic stress activates MAPKs, which may control the functions of check-point proteins in root meristem cells of *V. faba*; the MAPK-signaling pathway takes part in response to hydroxyurea-induced genotoxic stress (Winnicki and Maszewsky, 2012).

Because higher plants constitute the first level of the trophic chain and because they are exposed continuously in different environmental risk factors, is relevant and important to detect the changes that occur in those plants and to monitor the impact to human health that those have. For this reason the aim of the present study was to determine whether different concentrations of the OIs fenthion and malathion, and the HM salts nickel nitrate and potassium dichromate, could induce DNA damage (evaluated as comets) or alter the expression of AL-PCD in *A. cepa* and in *V. faba* roots.

2. MATERIALS AND METHODS

2.1 Plant material and chemical reagents

A. cepa bulbs were obtained by donation from the Cell Biology Laboratory of the Biology Research Center in Madrid, Spain (CIB). *V. faba* seeds were purchased in a regional market in México City. Both the bulbs and seeds where acquired as “organic”, which means they were not exposed to pesticides during their culture, transportation, or

storage. Two insecticides, fenthion and malathion (CAS number 73981-34-7 and 121.75-5, respectively), were purchased as commercial compounds. Fenthion, also known as lebaycid, was obtained from Agroterra and Cheminova Agro, S.A, Spain. Malathion, also known as malafin, was obtained from Inca Islas Canarias, Spain. Historesin 8100 was obtained from Kulzer. Potassium dichromate and nickel nitrate (CAS number 7778-50-9 and 13138-45-9, respectively) were purchased from Mallinckodt Baker, S.A. de C.V., México. All of the other reagents used were of analytical grade.

2.2. Treatments with the environmental agents

The onion bulbs were germinated for four days in tap water to induce root growth; the broad bean seeds were soaked and germinated inside a humid camera in darkness for five days to 19 ºC. To assess the potential genotoxic effect and PCD induction, the *A. cepa*-germinated bulbs and *the V. faba* seedlings were divided into two groups, with six bulbs or seedlings in each group. The following OI treatments were used: 0.075, 0.75 and 7.5 M solutions. The following HM treatments were used: 0.01, 0.02, 0.05, 0.1, 0.2, and 0.4 M potassium dichromate and nickel nitrate. Both plant-model treatments lasted 2 h. The selection of the OI and HM concentrations and exposure times used in the present study were based on the results of preliminary experiments. Negative controls remained in distilled water for the same amount of time as the exposed groups. After treatment, the roots were rinsed in tap water and 2.0 cm-cuts were made. One of the groups was maintained in cold phosphate saline buffer (PBS) at a pH of 7.4 (Dubelcco's PBS, sterilized, 1 liter per packet) until the isolation of nuclei (≤ 15 min). In the second group, 0.75-cm cuts were made and fixed overnight in 4% paraformaldehyde (PF) (weight/volume in PBS, pH 7.4). Later they were stored in 0.1% PF for PCD evaluation.

2.3. DNA damage (comet assay)

2.3.1. Isolation of nuclei from roots

The nuclei were isolated mechanically under dim or yellow light by placing the 2-cm root cuts in a 60 mm glass Petri dish, and 250 µL of cold PBS (pH 7.4) was poured onto each sample. Using a cold scalpel, the roots were sliced transversally into the buffer. The Petri dish was kept on ice so that the nuclei would collect by precipitation in the buffer. In

160 micro vials with 50 µL of molten low melting point agarose (LMPA), 50 µL of nuclei
161 suspension were added and pipetted repeatedly to gently mix the solution. Using a cut tip,
162 80 µL of the mixture were placed onto a cover slip (24 x 50 mm). A microscope slide with
163 frosted ends that had been previously covered on one side with 1.0% normal melting point
164 agarose (NMPA) was carefully connected, to avoid the formation of air bubbles. In order to
165 solidify the agarose, the slide was placed on a cold surface for a minimum of 5 min, after
166 which the cover slip was removed and a final layer of 80 µL of molten 0.5% LMPA was
167 placed on the slide and kept on a cold surface for 5 min.
168
169 *2.3.2. Lyses*
170 The cover slips were removed, and all of the slides were placed in a box with a flat
171 background containing cold (4 ^{o}C) lysis solution (2.5 M NaCl, 0.1 M EDTA, 10 mM Tris,
172 10N NaOH, 10% DMSO, and 1% Triton X-100 in deionized water; pH 10) for1 h in
173 darkness.
174
175 *2.3.3. Unwinding and electrophoresis*
176 All of the slides were drained vertically, the bottoms of the slides were dried to
177 remove the lyses solution, and the slides were placed in an electrophoresis chamber and
178 immersed in electrophoresis buffer (10 N NaOH and 200 mM EDTA; pH > 13). The nuclei
179 were incubated for 20 min to allow the DNA to unwind. Subsequently the electrophoresis
180 was conducted to 4 ºC putting the chamber inside a refrigerator in darkness at 0.74 V/cm
181 (25 V, 300 mA) for 20 min. After electrophoresis, the slides were neutralized three times
182 with 0.4 M Tris buffer (pH 7.4), stained or incubated for 15 min in cold ethanol, left
183 overnight to dry, and stored in slide boxes until they could be registered.
184
185 *2.3.4. Staining and comet scoring*
186 The slides were stained with 50 µL of 0.2 mg/mL ethidium bromide and covered
187 with a cover slip. Slides with stained nuclei were placed between two paper towel layers
188 that were soaked in 0.45 mM Millipore filtering water, to avoid contamination by bacteria
189 and to avoid dye evaporation. The slides were protected from the light using aluminum foil
190 to avoid the decrease of the fluorescence. The comets were scored within three or four

191 days. At least 50 cells for each slide and three slides per treatment were analyzed in an
192 epifluorescence Axiostar Plus Carl Zeiss microscope with an exciting filter of 515–560 nm
193 and a barrier filter of 590 nm. The computerized image analysis system, Comet Assay IV
194 (Perceptive Instruments), was used to measure DNA damage based on the tail moment.
195 Only the nuclei images that contained good structures and brightness intensity were
196 analyzed. All of the slides were coded before scoring to avoid bias.
197
198 **2.4. Analysis of programmed cell death**
199 *2.4.1. Processing of samples for structural, microscopic, and immunofluorescence analysis*
200 Groups of *A. cepa* and *V. faba* roots that were treated with pesticides and HMs and
201 that were stored in 0.1% PF were used one for inclusion in HistoResin and later structural
202 analysis. For this intention, they were washed three times for 5 min with PBS, they were
203 dehydrated with 30, 50% acetone for 1 h, and immersed overnight in 70% acetone.
204 Immediately, the samples were dehydrated in 90% acetone for 1 h and 100% acetone for 1
205 h three times; the whole procedure was realized at 4 ^{o}C. The roots were then immersed in
206 an infiltration solution of HistoResin 8100 at 4 ^{o}C and agitated in a rotator overnight. The
207 next day, the samples were placed in capsules with embedding solution, capped, and they
208 were left to polymerize to 4 °C. Semi-thin sections (1 μm thickness) were obtained and
209 stained with 0.5 (v/v) toluidine blue in distilled water for light microscopy analysis. The
210 stained semi-thin sections were observed under bright and phase contrast for structural
211 analysis using a microscope Leite fitted to an Olympus DP10 digital camera. Some sections
212 were stained with 4,6-diamine-2-phenyl-indole (DAPI; Serva, Heilderberg, Germany) and
213 observed under epifluorescence microscopy to visualize the nuclei. Other groups of
214 samples were used for direct sectioning using a vibratome, and additional
215 immunofluorescence procedures were carried out.
216
217 *2.4.2. Immunofluorescence and confocal laser microscopy*
218 Immunofluorescence was performed on vibratome sections, as previously described
219 (Fortes et al., 2004). Briefly, 30- μm vibratome sections (Vibratome 1000, Formely Lancer)
220 were obtained from fixed *A. cepa* and *V. faba* roots (see above), placed onto slices coated
221 with 3-aminopropyltrithoxysilane, and treated for permeabilization purposes. First, the

samples were dehydrated (30, 50, 70 and 100 % v/v in PBS: methanol) and rehydrated (100, 70, 50 and 30% v/v in PBS: methanol series). Next, the sections were treated with 2% (w/v) cellulase (Onozuka R-10) in PBS for 5 min, treated with 0.5% triton X-100 in PBS for 20 min, and washed with PBS for 5 min twice. Subsequently, sections were incubated with 5% (w/v) bovine serum albumin (BSA) in PBS for 5 min. They were then incubated in anti-cleaved caspase-3, anti-ERK, and anti-phospho-ERK polyclonal antibodies and anti-Cyt C monoclonal antibody, which had been diluted to 1:10, 1:25, 1:50, and 1:100, respectively, in 1.0% BSA for 1 h at room temperature. After washing twice with PBS for 10 min each, the signal was revealed with either ALEXA 488 (green fluorescence) or conjugated anti-rabbit and anti-mouse antibodies (Molecular Probes, Eugene, OR) that were diluted to 1:25 in 1% BSA for 1 h in darkness at room temperature. Finally, the sections were washed twice with PBS for 10 min, stained with DAPI for 10 min, washed with H_2O milli-Q, and mounted with Mowiol 4-88 (Polysciences, Eppelheim, Germany). Immunofluorescence assays were observed using confocal laser microscopy (CLSM) (Leica TCS-SP2-A=BS), and a Z-series of 0.5–1 μm optical sections were collected. Images were taken from projections of series of 15–20 optical sections. To allow an accurate comparison between signals of control cells and treated cells, confocal microscopy analysis was performed using the same laser excitation and sample emission capture settings in all immunofluorescence preparations of each species.

2.5. Statistical analysis

The comet assay evaluation was made by examining the tail moment (Olive tail moment) of each nucleus; this data included consideration of both the migration of the genetic material, which was determined by the tail length, and the relative amount of DNA, which was determined by the intensity of the comet tail. Data were analyzed using a variance analysis. When significant differences between the control group and each treated group were obtained, the Newman–Keuls comparison test was applied.

3. RESULTS

3.1. DNA damage (comet assay)

The results of the comet assay are presented in Fig. 1 and in Tables 1 and 2. Clear genotoxic effects following later to the treatment with the OIs and HMs were demonstrated in *A. cepa* (Fig. 1b) and in *V. faba* (Fig. 1e) roots (Tables 1 and 2) through the tail moment with relation to the control of A. cepa (Fig 1a) and A. cepa (Fig. 1d). Highest concentrations of potassium dichromate and nickel nitrate produced nuclei pulverization and cloud formation, whereby genetic material did not migrate during the electrophoresis but showed a round spherical form (Table 1; Figs. 1c, 1f). *A. cepa* roots were more sensitive to the chemical exposures compared to *V. faba* (Tables 1 and 2). A dose-dependent response was observed in the experiments presented here, and the DNA damage induced by OIs and HMs was significantly different compared to the controls for both plant models and at all concentrations studied.

3.2. Subcellular structural changes

DNA damage, characterized by the induction of comets in low dose and clouds in the highest concentrations, was correlated with the appearance of several structural characteristics of the AL-PCD process. Following exposure of *A. cepa* to OI and exposure of *V. faba* to HM, several signs of AL-PCD were evaluated, including chromatin condensation, vacuolization, nuclear lobes, condensation of the protoplast away from the cell wall, and fragmentation. Structural changes induced by OIs in *A. cepa* are presented in Figs 2e, 2f; similar changes were observed after HM treatments in *V. faba* (Figs. 2g, 2h) compared with *A. cepa* control (Figs 2a, b) and with *A. cepa* control (Figs 2c, 2d) both, dyeing with DAPI and toluidine, respectively. Moreover, nuclear fragmentation (Figs. 1c, 1f) and the formation of apoptotic bodies were observed in root cells of both plant models after highest treatments (Figs. 2i, 2j, 2k, and 2l).

3.3. Markers of programmed cell death

Features associated with AL-PCD under abiotic stress were used as molecular markers in the present study. Root cells treated with OIs showed similar alterations, such as the increased presence of active-caspase-3-like enzymes, in both *A. cepa* cells (Figs. 3f, 3h) and *V. faba* cells treated with HM (Figs. 3j, 3l) when compared with the respective controls (Figs. 3b, 3d).

Cyt C immunolocalization showed a punctuate pattern of localization in control cells, which corresponded to mitochondria, while in treated cells, the Cyt C signal appeared faint and diffuse in the cytoplasm. This observation suggested the release of Cyt C into the cytoplasm (Figs. 3r, 3v); this effect was observed mostly at the higher concentrations of the fenthion insecticide compared to the respective control of *A. cepa* (Fig. 3n). In *V. faba* cells treated with HMs (Figs. 3t, 3x), the same behavior was observed as for *A. cepa*; in this case, the signal was higher with Cr salt. All of the experimental scenarios are presented with DAPI-stained nuclei in Figs. 3a, 3c, 3e, 3g, 3i 3k, 3m, 3o, 3q, 3s, 3u, and 3w.

Another change observed after the OI and HM treatments was the significant decrease of ERK proteins with the highest concentrations of chemicals tested. This finding was observed mainly with *V. faba* cells exposed to HMs (Figs. 4j, 4l), and to a lesser extent with *A. cepa* exposed to OIs (Figs. 4f, 4h) in comparison with the respective controls (Figs. 4b, 4d).

Phospho-ERK proteins decreased similarly following OI exposure in *A. cepa* (Figs. 4r, 4t) and HM exposure in *V. faba* (Figs. 4v, 4x) compared to their respective controls (Figs. 3n, 3p). All of the experimental scenarios are presented with DAPI-stained nuclei in Figs. 4a, 4c, 4e, 4g, 4i, 4k, 4m, 4o, 4q, 4s, 4u, and 4w. Table 3 shows comparative behavior of AL-PCD markers induced by OI and HM in *A. cepa* and *V. faba*, respectively.

4. DISCUSSION

There are alternative approaches to study and evaluate the effects of environmental pollutants. In the present study, we explored the DNA damage and the induction of AL-PCD following exposure to OIs and HMs in two plant models, *A. cepa* and *V. faba.* Results obtained at the same time allowed us to investigate the way in which two different plant systems react to OIs and HMs, which can be useful for understanding the way in which other plant species respond to environmental pollutants.

Previous studies thoroughly analyzed the ability of some OIs to induce mutagenesis and genotoxicity in *A. cepa* (Bianchi et al., 2015; Pathiratne et al, 2015; Santos et al., 2015). Similarly, several researchers described genotoxic effects of environmental agents in *V. faba* (Arya et al., 2017; Hu et al., 2016; Igbal, 2016; Santos et al., 2015). DNA damage and chromatin pulverization induced in the root tips of both *A. cepa* and *V. faba* following

314 exposure to OIs and HMs in the present study are in agreement with Moore et al. (2010),
315 who found cytotoxic and genotoxic effects induced by the OI malathion in $HepG_2$ cells and
316 Paz-Trejo and Gómez-Arroyo (2017) in human lymphocytes. (Moore et al. (2010)
317 associated the cytotoxic and genotoxic effects with the formation of malondialdehyde, an
318 end-product of lipid peroxidation. These similarities suggest that oxidative stress plays an
319 important role in the damage produced by malathion and fenthion in the present research.
320 ROS caused oxidative stress by inhibiting antioxidant enzymes that are involved in
321 the toxicity of various pesticides, including OI. ROS induced several types of DNA lesions,
322 which were detected in the present study using a comet assay, including single- and double-
323 strand breaks, alkali labile sites, and various species of oxidized purines and pyrimidines
324 (Tice et al., 2000). There have been several attempts to establish the mechanism of OI-
325 induced DNA damage, but results have been inconsistent. However, most studies supported
326 the idea that oxidative stress mediated several types of damages that were induced by OI.
327 Some of those studies demonstrated indirect changes. For example, Alleva et al. (2016)
328 showed that malathion, among others OI, induced mitochondrial dysfunction and parallel
329 ROS formation from mitochondria (mtROS). Furthermore, in a residential population that
330 was chronically exposed to pesticides, consequent DNA damage was efficiently inhibited
331 by honey extracts that contained polyphenols; a marked reduction of pesticide-induced
332 DNA lesions was observed. Lu et al. (2012) observed significant attenuation of the
333 cytotoxic and genotoxic effects caused by malathion, among other OIs to PC12 cells. The
334 authors also observed a subsequent reversal in the OIs-induced elevation of peroxidation
335 products and a decline of antioxidant enzyme activities, indicating that oxidative damage is
336 likely to be an initiating event that contributes to OIs-induced cytotoxicity.
337 In the context of the HMs used in the present study, Fargašová (2012) reported a
338 relevant role for plants in the risk assessment of Cr and Ni. The results of Fargašová (2012)
339 showed that HMs caused a significant increase in chromosomal aberrations. Several studies
340 have revealed that HMs are capable of catalyzing oxidative deterioration of biomolecules
341 (Koedrith et al., 2013). Toxic metal ions with similar properties to essential ions (for
342 example, charge and size) may compete with essential ions for biological binding sites,
343 resulting in disturbances in the structure and function of several biomolecules, as well as an
344 imbalance in metal homeostasis (Beyersman and Hartwig, 2008; Koedrith and Seo, 2011).

345 Nickens et al. (2010) described a simple but outstanding spectrum of cellular effects caused
346 by Cr (VI). They reported that intracellular metabolism of Cr (VI) led to the formation of
347 Cr–DNA adducts, genomic damage and mutagenesis, ROS production, and alteration of
348 survival signaling pathways. Those researchers, like Tchounwou et al. (2012), state that
349 although the mechanisms of biological interactions of Cr are uncertain, the variation in
350 toxicity may be related to the ease with which Cr can pass through cell membranes. On the
351 other hand Wise et al. (2002) indicate a biological relevance of non-oxidative mechanisms
352 in Cr (VI) carcinogenesis. In the present study, Cr VI (chromium dichromate) showed
353 significant differences between the control and the treated groups in terms of DNA damage
354 and the dose-response patterns.

355 The Ni-induced genotoxicity observed in the present study, can be supported by
356 mechanisms previously described, Das and Buchner (2007) explained it by the depletion of
357 glutathione levels and the binding of proteins to sulfhydryl groups using vitamin C a
358 possible protective antioxidant. Cameron et al. (2011) carried out an extensive review of
359 molecular mechanisms of Ni-induced genotoxicity and carcinogenicity, and they reported
360 an interesting chain of events that occur up to the point when oxidative stress severely
361 damages DNA. The results of the present study are in agreement with several references
362 mentioned before, and we suggest an induced oxidative stress route because of the affinity
363 of both OI and HM compounds with DNA molecules.

364 Unfortunately, one limitation of our study was that we did not explore molecular
365 mechanisms or subcellular response pathways corresponding to HM genotoxicity.
366 However, genotoxicity assays showed a clear dose-dependent relationship up to a certain
367 threshold, after which pulverized chromatin was observed forming clouds that were a
368 spherical shape and that did not show migration.

369 PCD has been largely studied in animals, but remains poorly understood in plants.
370 The overall process of cell death has different morphological and biochemical features in
371 plants and animals. However, recent advances suggest that nuclear disassembly in plant
372 cells progresses with morphological and biochemical changes that are similar to those in
373 apoptotic animal cells. Dominguez and Cejudo (2012) summarized nuclear dismantling in
374 plant PCD, focusing on the similarities and differences with their animal counterparts.
375 Reape et al. (2008) used the term AL-PCD; the author acknowledged that there were

similarities between AL-PCD and apoptosis, while recognizing that there were distinct, and perhaps fundamental, differences (Reape and McCabe, 2010). In the present study, OIs and HMs induced several structural changes that were characteristic of AL-PCD, such as condensed chromatin, cytoplasmic vacuolization, shrunken nuclei, and DNA fragmentation with the formation of apoptotic-like bodies in root cells of *A. cepa* and *V. faba*. Using a colorimetric method, Rodríguez-Serrano et al. (2012) described an increase in cell death and caspase 3-like activity that was induced by cold stress in microspores of *Hordeum vulgare*. Solis et al. (2014) found the highest levels of caspase 3-like activity in the tapetum in *Brassica napus* and *Nicotiana tabacum* during developmental PCD, and changes in the subcellular location of Cyt C toward cytoplasm in tapetum cells during PCD. In active cells, Solis et al. (2014) identified Cyt C using a punctuate fluorescent signal in the cytoplasm that corresponded to the mitochondria, while the cells that initiated PCD also exhibited a faint diffuse fluorescent signal in their cytoplasm, indicating the partial release of Cyt C molecules to the cytoplasm; some similar behaviors were observed in the present study.

The MAPK pathways are involved in the regulation of diverse cellular events, including proliferation, differentiation, and apoptosis. Among them, the ERKs, which are activated by phosphorylation (PhERKs), have been associated with cytoprotective roles in most systems (Gao et al., 2011). In plants, ERK homologues have shown expression patterns consistent with a role in proliferative events, such as microspore embryogenesis initiation of various plant species (Coronado et al., 2002; Seguí-Simarro et al., 2005). In the present study the results showed that ERK proteins decreased significantly in highest concentrations of both OIs and HMs.

AL-PCD studies that use malathion and fenthion in plant systems are scarce. In the present study, one limitation was that we did not undertake any experiments that explored molecular mechanisms underlying AL-PCD. Nevertheless, structural changes induced by OIs and HMs are clear and agree with several features of apoptotic morphology observed in animal cells (Reape et al., 2008). Reape and McCabe (2010) observed distinctive morphology associated with animal apoptosis, such as cell shrinkage and nuclear condensation and fragmentation, which differentiates it from other types of cell death. Likewise, the condensation of the protoplast away from the cell wall and DNA degradation

407 are characteristic of AL-PCD. Bhardwaj and Saraf (2015) analyzed the effects of malathion
408 exposure on granulosa cells of caprine antral follicles by transmission electron microscopy,
409 and they described several similar structural changes, such as diminished cell-cell contact,
410 presence of crescent-shaped nuclei, chromatin condensation, pycnosis with nuclear
411 membrane folding, and the accumulation of lipid droplets that may likely be related with to
412 the large vacuoles observed in the present study. Karami-Mohajeri et al. (2014) described a
413 reduction in mitochondrial apoptotic signaling that may be due to a reduction in adenosine
414 triphosphate (ATP) and ROS and to the genotoxic potential of malathion. Some other
415 pesticides, such as the insecticide rotenone, stimulate apoptosis; the apoptotic effect of
416 rotenone is at least partially due to mitochondrial injury (Lupesco et al., 2012).
417 Chlorpyrifos (CPF) induced apoptosis in dopaminergic neuronal components of PC12 cells,
418 as demonstrated by the activation of caspases and nuclear condensation (Lee et al., 2012).
419 In addition, Lee et al. (2012) found that CPF treatment activated MAPK pathways,
420 including ERK 1/2, c-Jun N-terminal kinases (JKN), and the p38 MAP kinase in a time-
421 dependent manner. N-acetyl-cysteine (NAC) treatment abolished MAPK phosphorylation
422 caused by CPF, indicating that ROS are upstream signals of MAPK. Interestingly, MAPK
423 inhibitors abolished cytotoxicity and reduced ROS generation following CPF treatment.
424 Cr has been largely shown to induce cell arrest and apoptosis in human cells. Russo
425 et al. (2005) demonstrated that DNA-damage and phosphoprotein (p53) activation are
426 important intermediates of Cr-induced apoptosis. Antioxidants, such as vitamin C and
427 NAC, protect against Cr-induced cell death (Quinteros et al., 2008). Cr exposure has been
428 shown to induce caspase-dependent and caspase-independent apoptotic pathways (Chen et
429 al., 2001; Pulido and Parrish, 2003; Singh et al., 1998).
430 Caspase expression and the release of Cyt C induced by Cr and Ni treatments in the
431 present study were clear, and ERK and PhERK depletion allowed us to speculate about an
432 oxidative stress mechanism. Cameron et al. (2011) suggested that Ni compounds enter the
433 cell, activate the CaSR receptor, and trigger intracellular Ca^{2+} mobilization and induction of
434 the calcium hypoxia-inducible factor pathways. Furthermore, he suggested that Ni enters
435 the nucleus, directly binds to DNA, and reacts with H_2O_2 to form reactive Ni-oxygen
436 complexes, resulting in the oxidation of thymine and cytosine residues accompanied by 8-

437 OH-dG formation. The oxidative stress generated severely damage DNA and inhibited
438 DNA repair pathways.

439 Molecular mechanisms by which Ni compounds caused cellular damage are far
440 from being understood (Guan et al., 2007). Ni produces reactive oxygen species (ROS)
441 (*OH^-), lipid peroxidation, oxidative DNA damage, and glutathione (GSH) depletion
442 (Valko et al., 2005). The mechanisms for Ni-induced apoptosis have not been extensively
443 studied. An increase in FasL protein and caspase-3 activation has been reported to be
444 associated with Ni exposure; similarly, in the present study, we obtained a significant
445 increase in caspase-3-like expression.

446 A number of carcinogenic metals (including the two used in the present study,
447 which are known and possible human carcinogens) are associated with apoptosis, and a
448 potential role of ROS, the mitochondria, and activation of several signaling pathways
449 (including MAPK and p53) has been established for several metals. Like in the present
450 study, apoptosis must be considered more generally as an effect of heavy-metal exposure;
451 Pulido and Parrish (2003) and Guan et al. (2007) highlighted the role of apoptosis in the
452 overall response to metal exposure. Taj et al. (2010) discussed the role of MAPK pathway
453 modules in plant stress signaling. In mammals, DHA-induced apoptosis has been reported
454 to be associated with a process that involves ERK inactivation, culminating in cytochrome
455 C release and caspase activation (Gao et al., 2011). In the present work, a significant
456 decrease in the ERK and PERK signals was obtained following HM exposures; that
457 decrease was slightly greater following exposures to OIs, in addition to the release of Cyt C
458 and an increase in caspase 3-like proteins. Much research in the plant PCD field has
459 focused on the possible role of Cyt C and caspases in destruction of the cell. It is becoming
460 clear that while the mitochondria and caspase-like molecules play an important role in plant
461 AL-PCD, one effect of Cyt C release, from the mitochondria following a stress response, is
462 the production of ROS (Reape and McCabe 2010). There is growing evidence to support
463 the interaction between ROS and antioxidants as providing an interface for metabolic and
464 environmental signals that can modulate the induction of a cell's acclimation to stress or,
465 alternatively, activation of PCD (Foyer and Noctor, 2005). Taj et al. (2010) concluded that
466 there was a need to design novel approaches and strategies to define specific functions and
467 to elucidate the underlying mechanisms of signal transduction through the identification

and validation of functional plant MAPK components. Further, disorders of apoptosis may play a critical role in some of the most debilitating metal-induced afflictions, including hepatotoxicity, renal toxicity, neurotoxicity, autoimmunity, and carcinogenesis. An understanding of metal-induced apoptosis will be helpful in the development of preventive molecular strategies.

Obviously, during environmental toxicities induced by pollutants or toxicants, apoptosis plays a transcendental role in both removing damaged cells and in the pathophysiology of distinct environment-associated disease conditions. Interestingly, environmental stressors also induce the activation of survival responses—including DNA repair mechanisms, MAPK signaling cascades, and up-regulation of antioxidant defenses—in an attempt to counteract the deleterious effects of cell-death pathways, depending on the intensity, length, and type of exposure.

Franco et al. (2009) published an interesting review in which he concluded that redox signaling (that involves both alterations in antioxidant defenses and accumulation of ROS, leading to oxidative stress) is one of the central mechanisms by which many environmental stressors modulate or trigger apoptosis. The biochemical events mediated a number of redox-dependent processes, such as oxidative protein modifications; oxidative DNA damage and alterations in mitochondrial function can, in turn, trigger the activation of specific signaling cascades. Future research on the understanding of both environmentally-induced genotoxicity and apoptosis and environmentally-induced cellular transformation are necessary for a complete understanding of human health consequences of environmental exposures.

5. CONCLUSIONS

The present study emphasized the valuable role of two plants, *Allium cepa* and *Vicia faba*, as excellent test models for biological assays. This is because plants are highly sensitive, inexpensive, and easy to manage in studies of environmental pollutants, such as OIs and HMs. The evident ability of both types if chemicals (that is, OIs and HMs) to induce genotoxicity is shown by the significant increase in DNA damage, evaluated by the tail moment of comets. Furthermore, in the present study, the apoptotic-like changes that were produced increased the presence of active caspase-3-like proteins, increased the

release of Cyt C toward the cytoplasm, and decreased levels of ERK and PhERK proteins. Our results, which suggest a role for oxidative stress via underlying genotoxicity and on the basis of observed AL-PCD features, demonstrate a high affinity of both OI and HM compounds to DNA molecules. Consequently, this study highlighted the relevance of genotoxicity and AL-PCD induction as useful biomarkers of stress caused by exposure of *A. cepa* and *V. faba* root cells to both OIs and HMs and, in general, as early indicators of chronic stress induced by environmental pollution stressors.

CONFLICT OF INTEREST

The authors declare that there are no conflicts of interest.

Acknowledgements

The authors appreciate to Ministerio de Educación y Ciencia de España supports program by fellow shift to Josefina Cortés Eslava for search stay in sabbatical year (SAB 2003-0229) and to Programa de Intercambio Académico de la Universidad Nacional Autónoma de México-Consejo Superior de Investigaciones Científicas de España (UNAM-CSIC). We also thank to Claudio Amescua for his editing assistance and to Pietro Villalobos for the figures editing.

REFERENCES

Alleva, R., Manzella, N., Gaetani, S., Ciarapica, V., Bracci, M., Caboni, M.F., Pasini, F., Monaco, F., Amati, M., Borghi, B., Tomasetti, M. 2016. Organic honey supplementation reverses pesticide-induced genotoxicity by modulation DNA damage response. Mol. Nutr. Food Res. 00, 1-13.

Arya, S.K., Ghosh, I., Banerjee, R., Mukherjee, A. 2017. Malathion and dithane induce damage in *Vicia faba*. Toxicol. Ind. Health 33, 843-854.

Berrada, H., Fernández, M., Ruiz M.J., Moltó J.C., Mañes J. 2006. Exposure assessment of fruits contaminated. Food Addit. Contam. 23, 674-682.

Beyersmann, D., Hartwig, A. 2008. Carcinogenic metal compounds: recent insight into molecular and cellular mechanisms. Arch. Toxicol. 82, 493-512.

Bhardwaj, J., Saraf, P. 2015. Transmission electron microscopic analysis of malathion-induced cytotoxicity in granulosa cells of caprine antral follicles. Ultrastruct. Path. 40, 43-50.

Bianchi, J., Mantovani, M.S., Marin-Morales, M.A. 2015. Analysis of the genotoxic

potential of low concentrations of malathion on the *Allium cepa* cells and rat hepatoma tissue culture. J. Environ. Sci. 36,102-111.

Cameron, K.S., Buchner, V., Tchounwou, P.B. 2011. Exploring the molecular mechanisms of nickel-induced genotoxicity and carcinogenicity: A literature review. Rev. Environ. Health 26, 81-92.

Chen, F., Vallyathan, V., Castranova, C.V., Shi, X. 2001. Cell apoptosis induced by carcinogenic metals. Mol. Cell Biochem. 222, 183-188.

Chervona, Y., Costa, M. 2012. The control of histone methylation and gene expression by oxidative stress, hypoxia, and metals. Free Radic. Biol. Med. 53, 1041-1047.

Coronado, M.J., González-Melendi, P., Seguí, J.M., Ramírez, C., Bárány, I., Testillano, P.S., Risueño M.C. 2002. MAPKs entry into the nucleus at specific interchromatin domains in plant differentiation and proliferation processes. J. Struct. Biol. 140, 200-213.

Cortés-Eslava, J., Gómez-Arroyo, S., Arenas-Huertero, F., Díaz-Hernández, M.E., Calderón-Segura, M.E., Valencia-Quintana, R., Espinosa-Aguirre, J.J., Villalobos-Pietrini, R. 2013. The role of plant metabolism in the mutagenic and cytotoxic effects of four organophosphorus insecticides in *Salmonella typhimurium* and in human cells. Chemosphere 92, 1117-1125.

Das, K.K., Buchner, V. 2007. Effect of nickel exposure on peripheral tissues: role of oxidative stress in toxicity and possible protection by ascorbic acid. Rev. Environ. Health 22, 157-173.

Domínguez, F., Cejudo, F.J. 2012. A comparison between nuclear dismantling during plant and animal programmed cell death. Plant Sci. 197,114-121.

Fargašová, A. 2012. Plants as models for chromium and nickel risk assessment. Ecotoxicology 21, 1476-1483.

Foyer, C.H., Noctor, G. 2005. Redox homeostasis and antioxidant signaling: a metabolic interface between stress perception and physiological responses. Plant Cell. 17, 1866-1875.

Franco, R., Sánchez-Olea, R., Reyes-Reyes, E.M., Panayiotides M.I. 2009. Environmental toxicity, oxidative stress and apoptosis: Ménage à Trois. Mutat. Res. 674, 3-22.

Gichner, T., Plewa, M.J. 1998. Induction of somatic DNA damage as measured by single cell gel electrophoresis and point mutation in leaves of tobacco plants. Mutat. Res. 401, 143-152.

Gao, N., Budhraja, A., Cheng, S., Liu, E-H., Huang, Ch., Chen, J., Yang, Z., Chen, D., Zhang, Z., Shi, X. 2011. Interruption of the MEK/ERK signaling cascade promotes dihydroartemisinin-induced apoptosis *in vitro* and *in vivo*. Apoptosis 16, 511-523.

Guan, F., Zhang, D., Wang, X., Chen, J. 2007. Nitric oxide and bcl-2 mediated the apoptosis induced by nickel (II) in human T hibridoma cells. Toxicol. Appl. Pharmacol. 221, 86-94.

Hu, Y., Tan, L., Zhang, S.H., Zuo, Y.T., Han, X., Liu, N., Lu, W.Q., Liu, A.L. 2016. Detection of genotoxic effects of drinking water disinfection using *Vicia faba* bioassay. Environ. Sci. Pollut. Res. Int. 24, 1509-1517.

Igbal, M. 2016. *Vicia faba* bioassay for environmental toxicity monitoring: A review. Chemosphere 1441, 785-802.

Karami-Mohajeri, S., Hadian, M.R., Fouladdel, S., Azizi, E., Ghahramani, M.H., Hosseini

R, Abdollahi, M. 2014. Mechanisms of muscular electrophysiological and mitochondrial dysfunction following exposure to malathion, an organophosphorus pesticide. Hum. Exp. Toxicol. 33, 251-263.

Koedrith, P, Seo, Y.R. 2011. Advances in carcinogenic metal toxicity and potential molecular markers. Int. J. Mol. Sci. 12, 9576-9595.

Koedrith, P., Kim, H., Weon J.I., Seo Y.R. 2013. Toxicogenomic approaches for understanding molecular mechanisms of heavy metal mutagenicity and carcinogenicity. Int. J. Hyg. Environ. Health 216, 587-598.

Koppen, G. and Verschaeve, L. 1996. The alkaline comet test on plant cells: a new genotoxicity test for DNA strand breaks in *Vicia faba* root cells. Mutat. Res. 360,193-200.

Kuo, C.Y., Wong, R.H., Lin, J.Y., Lai, J.C., Lee, H. 2006. Accumulation of chromium and nickel metals in lung tumors from lung cancer patients in Taiwan. J. Toxicol. Environ. Health Part A 69, 1337-1344.

Lee, J.E., Park, J.H., Shin, I.C., Koh, H.C. 2012. Reactive oxygen species regulated mithochondria-mediated apoptosis in PC12 cells exposed to chlorpyrifos. Toxicol. Appl. Pharmacol. 263, 148-62.

Lockshin, R.A., Zakeri, Z. 2004. Apoptosis, autophagy and more. Biochem. Cell Biol. 36, 2405-2419.

Lou, J., Jin, L., Wu, N., Tan, Y., Song, Y., Gao, M., Liu, K., Zhang, X., He, J. 2013. DNA damage and oxidative stress in human lymphoblastoid cells after combined exposure to hexavalent chromium and nickel compounds. Food Chem. Toxicol. 55, 533-540.

Lu, X.T., Ma, Y., Wang, C., Zhang, X.F., Jin, D.Q., Huang, C.J. 2012. Cytotoxicity and DNA damage of five organophosphorus pesticides mediated by oxidative stress in PC 12 cells and protection by vitamin E. J. Environ. Sci. Health B. 47, 445-454.

Lupesco, A., Jilani, K., Zbidah, M., Lang, F. (2012). Induction of apoptotic erythrocyte death by rotenone. Toxicology 300, 132-137.

Ma, T.H. 1999. The role of plant systems for the detection of environmental mutagens and carcinogens. Mutat. Res. 437, 97-100.

Møller, P., Hemmingsen, J.G., Jensen, D.M., Danielsen, P.H., Karottki, D.G., Jantzen, K., Rousgaard, M., Cao, Y., Kermanizadeh, A., Klingberg, H., Christophersen, D.V., Hersoug, L.G., Loft, S. 2015. Applications of the comet assay in particle toxicology: air pollution and engineered nanomaterials exposure. Mutagenesis 30, 67-83.

Moore, P.D., Yedjou, C.G., Tchounwou, P.B. 2010. Malathion-induced oxidative stress, cytotoxicity and genotoxicity in human liver carcinoma (HepG2) cells. Environ.Toxicol. 25, 221-226.

Navarrete, M.H., Carrera, P., de Miguel, M., de la Torre, C. 1997. A fast comet assay variant for solid tissue cells. The assessment of DNA damages in higher plants. Mutat. Res. 398, 271-277.

Nickens, K.P., Petierno, S.R., Ceryac, S. 2010. Chromium genotoxicity: a double-edged sword. Chem. Biol. Interact. 188, 276-288.

Palaniappan, P.L., Karthieyan, S., 2009. Bioaccumulation and depuration of chromium in the selected organs and whole tissues of freshwater fish *Cirrhinus mrigala* individually and in binary solutions with nickel. J. Environ. Sci. 21, 229-236.

630 Panda B.B., Achary V.M.M. 2014. Mitogen-activated protein kinase signal transduction
631 and DNA repair network are involved in aluminum-induced DNA damage and
632 adaptative response in root cells of *Allium cepa*. Front. Plant Sci. 5, 256.
633 Pathiratne, A., Hemachandra, C.K., De Silva, N. 2015. Efficacy of *Allium cepa* test system
634 for screening cytotoxicity and genotoxicity of industrial effluents originated from
635 different industrial activities. Environ. Monit. Assess. 187,730
636 https://doi.org/10.1007/s10661-015-4954-z.
637
638 Paz-Trejo, C., Gómez-Arroyo, S. 2017. Genotoxic evaluation of common commercial pesticides in
639 human peripheral blood lymphocytes. Toxicol. Ind. Health 33, 938-945.
640 Pulido, M.D., Parrish, A.R. 2003. Metal-induced apoptosis: mechanisms. Mutat. Res. 533,
641 227-241.
642 Quinteros, F.A. Machiavelli, L.I., Cabilla, J.P., Dubilansky, B.H. 2008. Mechanisms of
643 chromium (VI)-induced apoptosis in anterior pituitary cells. Toxicology 294, 2-3.
644 Rana, S.V. 2008. Metals and apoptosis. J. Trace Elem. Med. Biol. 22, 262-284.
645 Reape, T.J., Molony, E.M., McCabe, P.F. 2008. Programmed cell death in plants:
646 distinguishing between different modes. J. Exp. Bot. 3, 435-444.
647 Reape, T.J., McCabe, P.F. 2010. Apoptotic-like regulation of programmed cell death in
648 plants. Apoptosis 15, 249-256.
649 Rodríguez-Serrano, M., Barany. I., Prem, D., Coronado, M.J., Risueño, M.C., Testillano,
650 P.S. 2012. NO, ROS, and cell death associated with caspase-like activity increases
651 in stress-induced microspore embryogenesis of barley. J. Exp. Bot. 63, 2007-2024.
652 Russo, P., Catassi, A., Cesario, A., Imperatori, A., Rotolo, N., Fini, M., Granone, P.,
653 Dominioni, L. 2005. Molecular mechanisms of hexavalent chromium-induced
654 apoptosis in human bronchoalveolar cells. A. J. Respir. Cell Biol. 33, 589-600.
655 Santos, C.L., Pourrut, B., Ferreira de Oliveira, J.M. 2015. The use of comet assay in plant
656 toxicology: recent advances. Front. Genet. 6, 216.
657 Seguí-Simarro, J.M., Testillano, P.S. Jouannic, S., Henry, Y., Risueño, M.C. 2005.
658 Mitogen-activated protein kinases are developmentally regulated during stress-
659 induced microspore embryogenesis in *Brassica napus* L. Histochem. Cell Biol. 123,
660 541-551.
661 Singh, J., Carlisle, D.L., Pritchard, D.E., Patierno, S.R. 1998. Chromium-induced
662 Genotoxicity and apoptosis: relationship to chromium carcinogenesis. Oncol. Rep.
663 5, 1307-1318.
664 Slotkin, T.A., Seidler, F.J. 2012. Developmental neurotoxicity of organophosphates targets
665 cell cycle and apoptosis, revealed by transcriptional profiles *in vivo* and *in vitr*o.
666 Neurotoxicol. Teratol. 34, 232-241.
667 Solis, M.T., Chakrabarti, N., Corredor, E., Cortés-Eslava, J., Rodríguez-Serrano, M.,
668 Biggiogera, M., Risueño, M.C., Testillano, P.S. 2014. Epigenetic changes
669 accompany developmental programmed cell death in tapetum cells. Plant Cell
670 Physiol. 55, 16-29.
671 Taj, G., Agarwal, P., Grant, M., Kumar, A. 2010. MAPK machinery in plants: recognition
672 and response to different stresses through multiple signal transduction pathways.
673 Plant Signal Behav. 5, 1370-1380.
674 Tchounwou, P.B., Yedjou, C.G., Patlolla, A.K., Sutton, D.J. 2012. Heavy metals and the
675 environment. Mol. Clin. Environ. Toxicol. Vol 3: Environ. Toxicol. Experientia
676 Supp. p. 133-164.

Tice, R.R., Agurell, E., Anderson, D., Burlinson, B., Hartmann, A., Kobayashi, H., Miyamae, Y., Rojas, E., Ryu, J,C,, Sasaky, Y.F. 2000. Single cell gel/comet assay: Guidelines *in vitro* and *in vivo* genetic toxicology testing. Environ. Mol. Mutagen. 35, 206-221.

Tsatsakis, A.M., Tzatzarakis, M.N., Tutudaki, M. 2008. Pesticide levels in head hair samples of Cretan population as an indicator of present and past exposure. Forensic. Sci. Int.176, 67-71.

Valko, M., Morris, H., Cronin, M.T. 2005. Metals, toxicity and oxidative stress. Curr. Med. Chem. 12, 1161-1208.

van Doorn, W.G., Beers, E.P., Dangl, J.L., Franklin-Tong, V.E., Gallois, P., Hara-Nishimura, I., Jones, A.M., Kawai-Yamada, M., Lam, E., Mundy, J., Mur, L.A., Petersen, M., Smertenko, A., Taliansky, M., Van Breusegen, F., Wolpwert, T., Woltering, E., Zhivotovsky, B., Bozhkov, P.V. 2011. Morphological classification of plant cell deaths. Cell Death Differ. 18, 1241-1246.

Winnicki K., Maszewski J. 2012. SB202190 affects cell response to hydroxyurea-induced genotoxic stress in root meristems of *Vicia faba*. Plant Physiol. Biochem. 60, 129-136.

Wise, J.P., Wise, S.S., Little, J.E. 2002. The cytotoxicity and genotoxicity of particulate and soluble hexavalent chromium in human lung cells. Mutat. Res. 517, 221-229.

Table 1. Effect of potassium dichromate and nickel nitrate in *Allium cepa* and in *Vicia faba* evaluated through comet assay.

	[a]Tail moment X ± S.E.	
	Allium cepa	*Vicia faba*
Negative control distilled water	0.6 ± 0.6	0.3 ± 0.1
Potassium dichromate [M]		
0.01	3.8 ± 1.0 *	1.5 ± 5.0*
0.02	6.2 ± 1.0 *	8.9 ± 3.2*
0.05	25.3 ± 4.1*	11.0 ± 1.3*
0.1	39.8 ± 6.4*	16.0 ± 6.8*
0.2	51.9 ± 8.6*	31.0 ± 12.0*
0.4	clouds[&]	clouds[&]
Nickel nitrate [M]		
0.01	2.4 ± 0.5*	1.7 ± 0.5 *
0.02	5.2 ± 0.4*	5.2± 1.7*
0.05	13.5 ± 5.3*	8.0 ± 1.2*
0.1	23.6 ± 8.6*	10.9 ± 3.1*
0.2	39.4± 6.8*	24.5 ± 5.8*
0.4	clouds[&]	clouds [&]

[a] Mean of at least two independent assays ± S.E.
n = 150 analyzed nuclei
* Significant differences were obtained by analysis of variance $F_{Allium\ cepa} = 476.6$, $F_{Vicia\ faba} = 982.6$ and therefore, the Newman-Keuls multiple comparison test was applied, $P < 0.001$.
[&] pulverized chromatin was observed forming a cloud that did not showed migration but spherical shape.

Table 2. Effect of fenthion and malathion in *Allium cepa* and in *Vicia faba* evaluated through comet assay.

	[a]Tail moment X ± S.E.	
	Allium cepa	*Vicia faba*
Negative control distilled water	0.8 ± 0.7	0.5 ± 0.5
Fenthion [M]		
0.057	37.1 ± 6.4 *	15.8 ± 6.8*

0.57	50.0 ± 10.1 *	33.5 ± 3.4*
5.7	clouds&	clouds&
Malathion [M]		
0.075	20.5 ± 8.6 *	13.6 ± 4.2 *
0.75	40.0 ± 9.3 *	25.0 ± 9.1*
7.5	clouds &	clouds&

[a] Mean of at least two independent assays ± S.E.
n = 150 analyzed nuclei
* Significant differences were obtained by analysis of variance $F_{Allium\ cepa} = 1456.2$, $F_{Vicia\ faba} = 976.3$ and therefore, the Newman-Kewls multiple comparison test was applied, $P < 0.001$.
& pulverized chromatin was observed forming a cloud that did not showed migration but spherical shape.

Table 3. Apoptotic-like programmed cell death (AL-PCD) markers induced by insecticides and heavy metals in *Allium cepa* and in *Vicia faba* respectively.

	Caspase 3-like	Cytochrome c	ERK	PERK
	Allium cepa			
Control	-	+ (punctate pattern:mitochondria)	+++	+++
Phention	+++	+ (difusse pattern:release to cytoplasm)	±	-
Malathion	+++	++ (difusse pattern:release to cytoplasm)	±	-
	Vicia faba			
Control	±	+ (punctate pattern:mitochondria)	++	+++
Nickel	++	++ (difusse pattern:release to cytoplasm)	-	-
Chromium	++	++ (difusse pattern:release to cytoplasm)	--	--

- There is not marker expression
± There is a sligth signal
+ The signal is more visible
++ The signal is very much evident
+++ The signal appear strongest

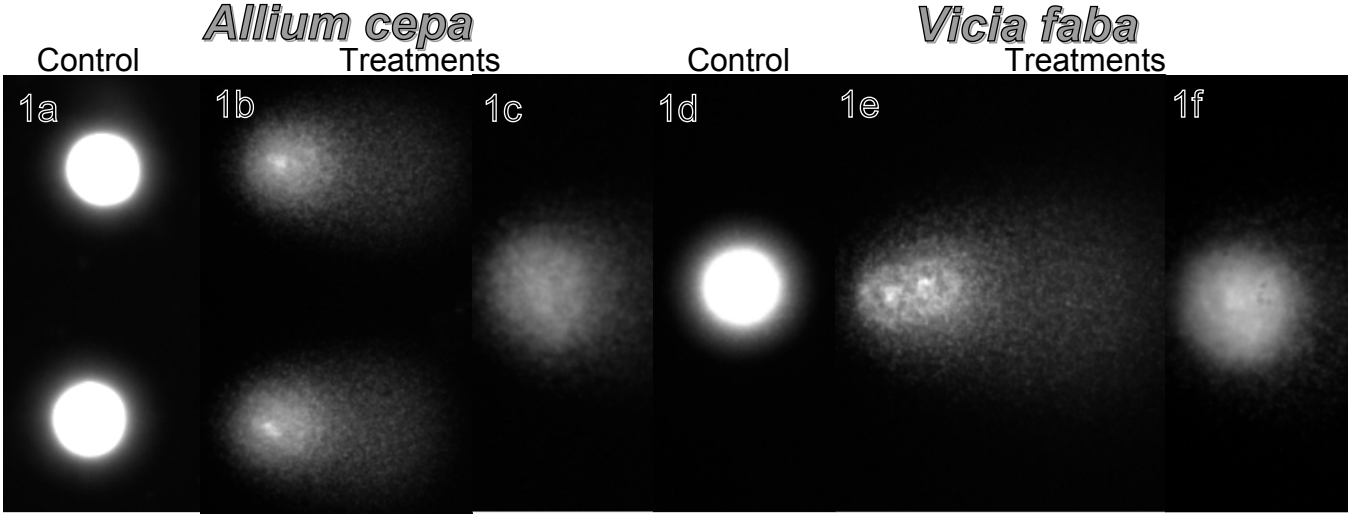
Allium cepa
Vicia faba
Control
Treatments
Control
Treatments
1a
1b
1c
1d
1e
1f

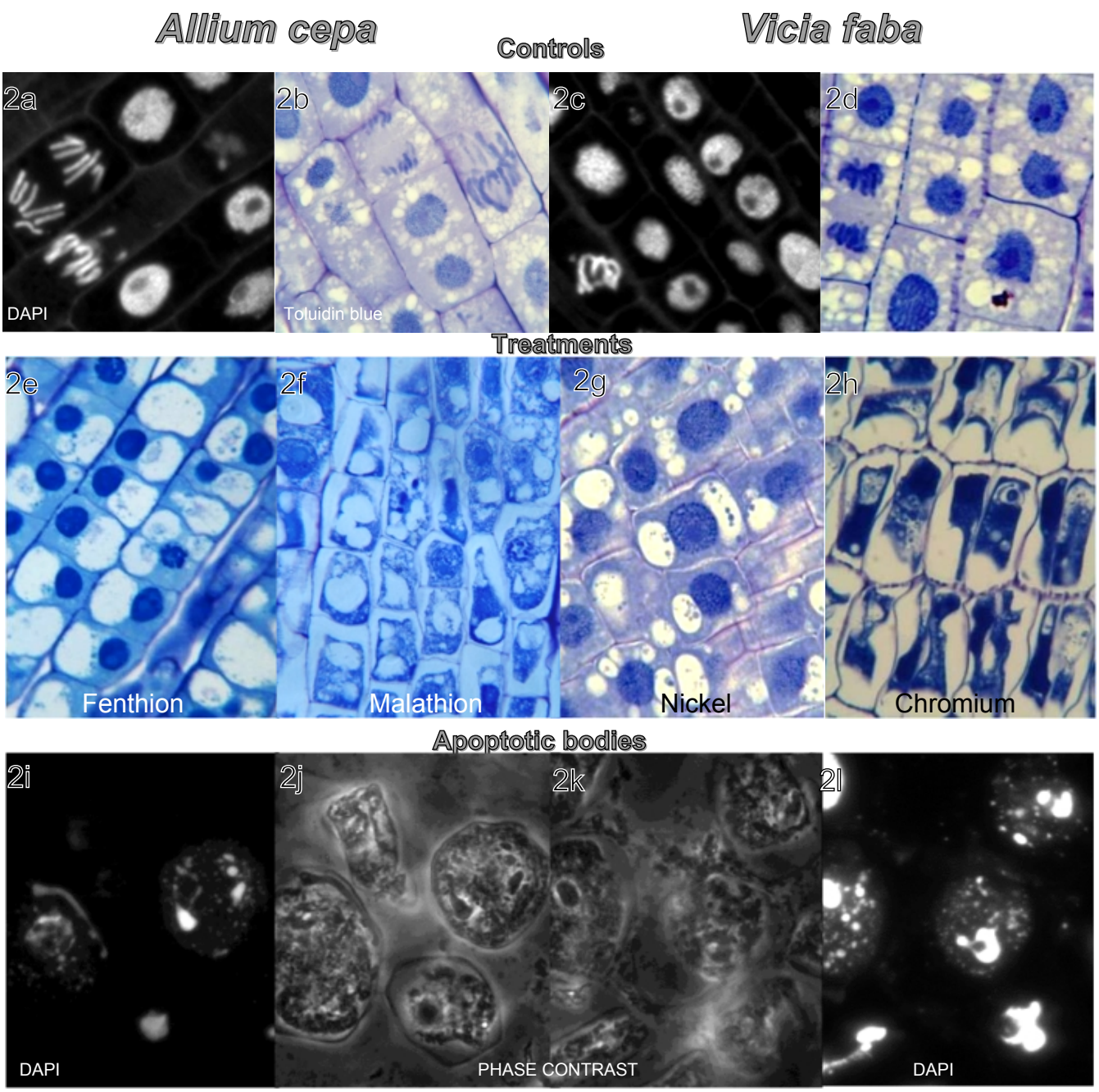
Allium cepa
Vicia faba
Controls
2a
DAPI
2b
Toluidin blue
2c
2d
Treatments
2e
Fenthion
2f
Malathion
2g
Nickel
2h
Chromium
Apoptotic bodies
2i
DAPI
2j
PHASE CONTRAST
2k
2l
DAPI

Allium cepa *Vicia faba*

Caspase 3-Like active

Controls

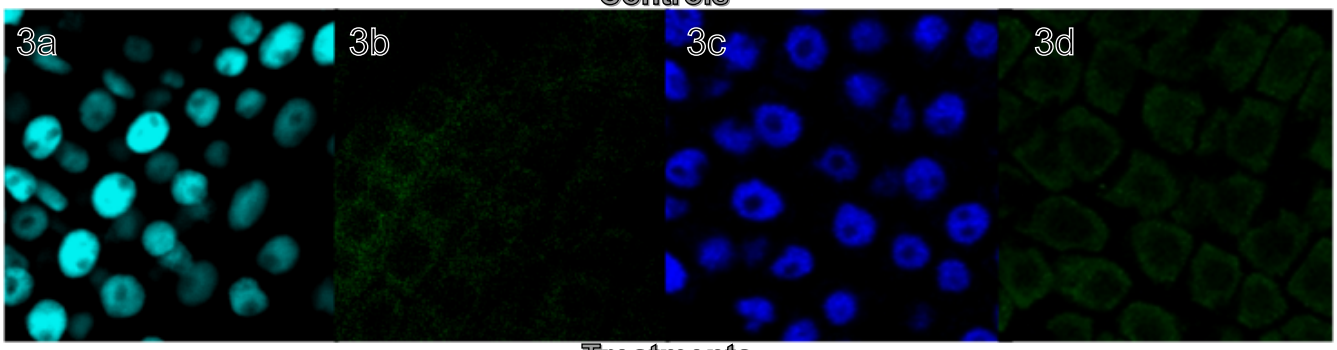

Treatments

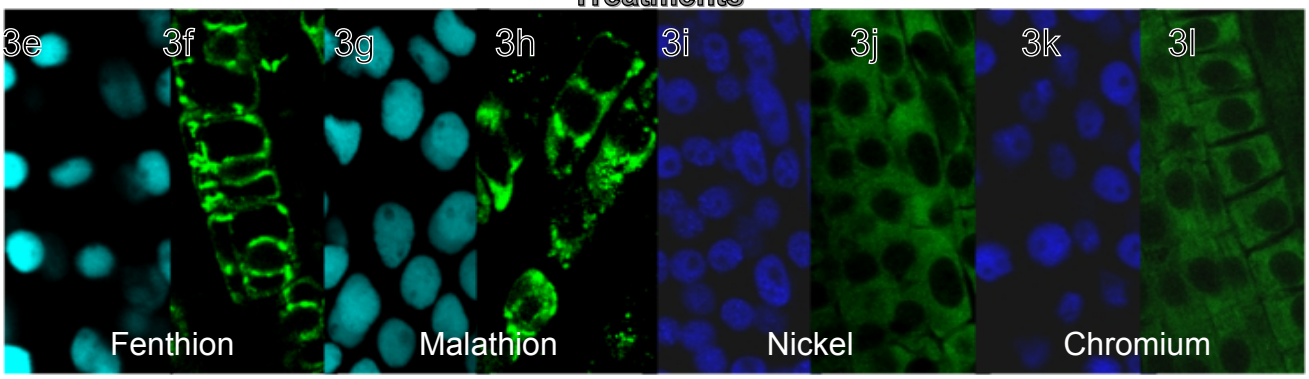

Cytochrome C

Controls

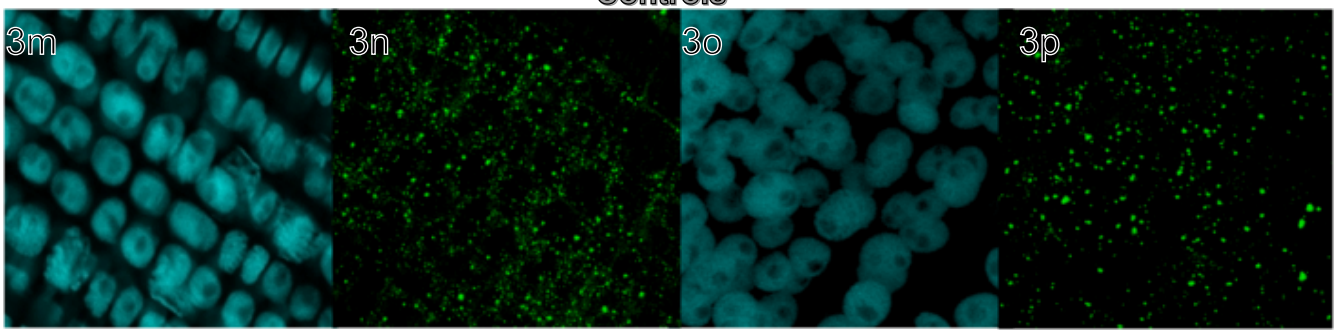

Treatments

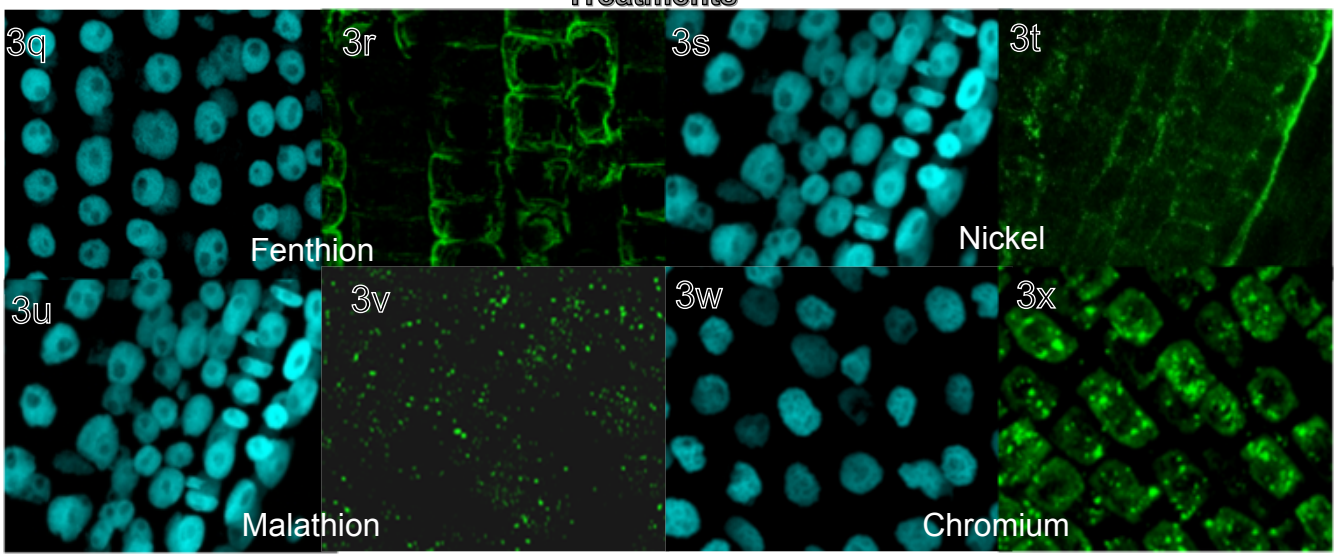

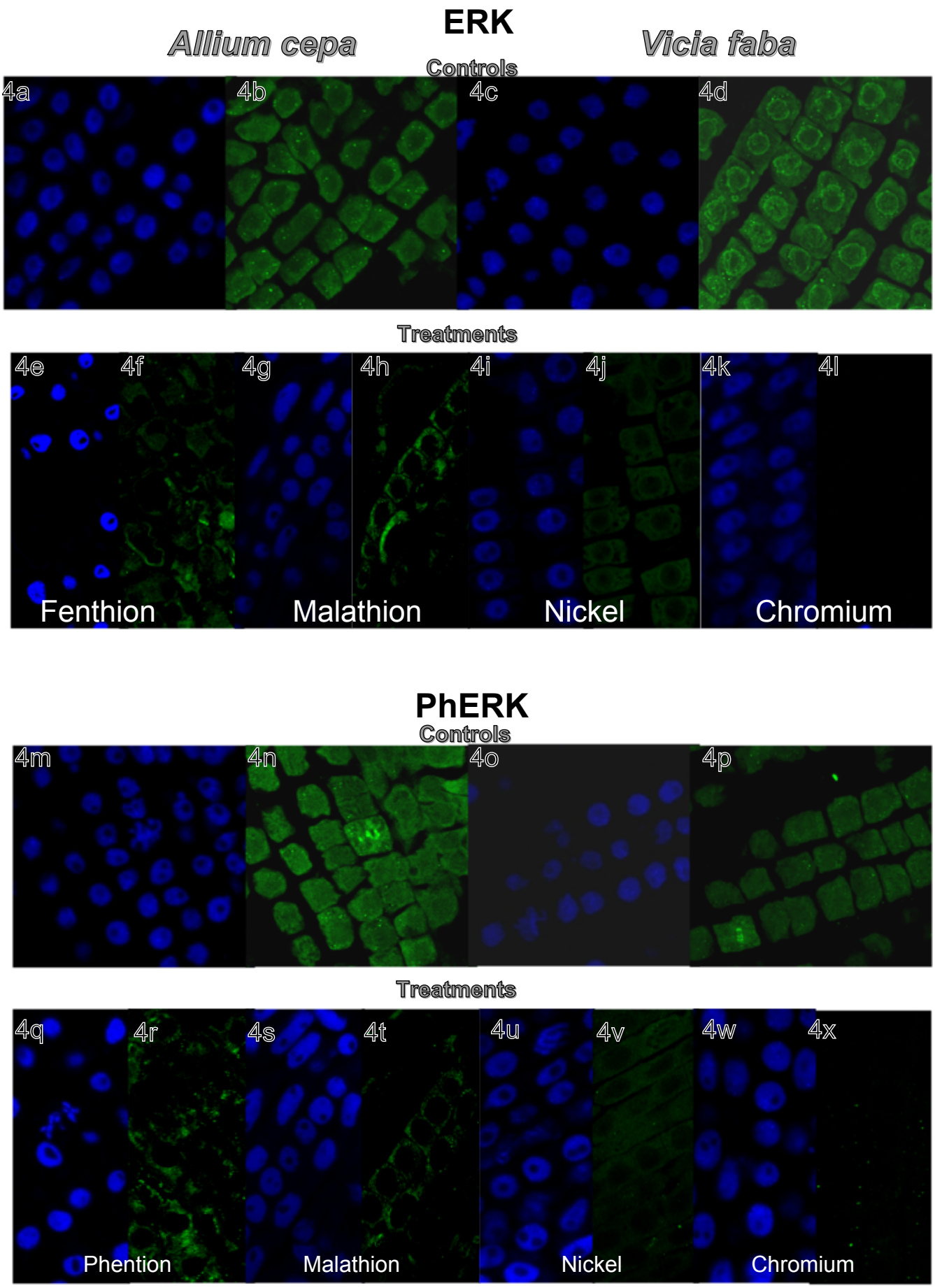
ERK
Allium cepa
Vicia faba
Controls
4a
4b
4c
4d
Treatments
4e
4f
4g
4h
4i
4j
4k
4l
Fenthion
Malathion
Nickel
Chromium
PhERK
Controls
4m
4n
4o
4p
Treatments
4q
4r
4s
4t
4u
4v
4w
4x
Phention
Malathion
Nickel
Chromium

FIGURE CAPTIONS

Fig. 1 Genotoxicity induced by insecticides and heavy metals in *V. faba* (1a-control, b-comet, c-cloud) and in *Allium cepa* (d-control, e-comet, f-cloud) in ethidium bromide staining slides.

Fig. 2 Structural changes and apoptotic-like bodies induction in toluidine blue and DAPI semi-thin sections of A. *cepa* (2a, b controls, e, f, i, j treatments) and of *V. faba* (2c, d controls, g, h, k, and l treatments).

Fig. 3 AL-PCD markers. Caspase 3-like enzymatic activity induced in *A. cepa* by insecticides (3a, b-control, 3e, f-7.5 M fenthion; 3g, h-7.5 M malathion) and in *V. faba* by heavy metals (3c, d-control; 3i, j-0.4 M nickel; 3k, l-0.2 M chromium). Immunolocalization of Cytochrome C in *A. cepa* (3m, n-control, 3q, r-7.5 M fenthion; 3u, v-7.5 malathion) and in *V. faba* (3o, p-control; 3s, t-0.4 M nickel nitrate; 3w, x-0.4 M potassium dichromate). The immunofluorescence signal (green) in control cells is punctate corresponding to mitocondrial localization whereas the signal is punctate and diffuse in the cytoplasm in treated cells, indicating the partial release of Cyt C into the cytoplasm at PCD; DAPI staining shows the nuclei (blue).

Fig. 4 Cellular enzymes involved in proliferation modified by heavy metals and insecticides: ERK in *A. cepa* (4a, b-control, 4e, f-7.5 fenthion; 4g, h-7.5 malathion) and in *V. faba* (4c, d- control; 4i, j-0.4 M nickel nitrate; 4k, l-0.4 M potassium dichromate. PhERK in *A. cepa* (4m, n-control; 4q, r-7.5 M fenthion; 4s, t-7.5 M malathion) and in *V. faba* (4o, p-control; 4u, v-0.4 M nickel nitrate; 4w, x-0.4 M potassium dichromate). Total ERK and PhERK immunofluorescence (green) and DAPI staining of nuclei (blue).